Effects of DNA Structure on Oxopropenylation by the Endogenous Mutagens Malondialdehyde and Base Propenal†

John P. Plastaras,‡ Peter C. Dedon,§ and Lawrence J. Marnett*,‡

A. B. Hancock Jr. Memorial Laboratory for Cancer Research, Departments of Biochemistry and Chemistry, Center in Molecular Toxicology and The Vanderbilt-Ingram Cancer Center, Vanderbilt University School of Medicine, Nashville, Tennessee 37232, and Division of Bioengineering and Environmental Health, Massachusetts Institute of Technology, 56-787, Cambridge, Massachusetts 02139

Received June 21, 2001

ABSTRACT: Malondialdehyde (MDA) and nucleobase propenals can transfer oxopropenyl groups to guanine residues of DNA to yield pyrimodopurinone (M_1G) adducts. The DNA structural requirements for reaction with α,β-unsaturated aldehydes were explored. We found that single-stranded DNA is more sensitive to oxopropenylation than double-stranded DNA, and supercoiled plasmid DNA is more sensitive than linearized plasmid DNA. Increasing ionic strength inhibits oxopropenylation, especially by adenine propenal. The intercalating agents ethidium bromide and 9-aminoacridine enhanced oxopropenylation by severalfold. In contrast, actinomycin D, which both intercalates and binds in the minor groove, inhibited oxopropenylation. The anthracycline drugs daunorubicin and doxorubicin enhanced oxopropenylation by MDA up to 3-fold and by adenine propenal up to 7-fold in a concentration-dependent manner. The minor groove binders netropsin and distamycin inhibited oxopropenylation, but methyl green, a major groove binder, had little effect. These data suggest that steric access to the target nucleophile located in the minor groove of DNA is critical for adduct formation by the endogenous mutagens MDA and base propenals.

Malondialdehyde (MDA)[1] is an endogenous product of lipid peroxidation that is carcinogenic in rats and mutagenic in bacterial and mammalian cells (*1*−*4*). MDA forms adducts with adenine and cytosine, but it reacts most readily with guanine to form a 1:1 adduct, pyrimidopurinone (M_1G) (Scheme 1) (*2*, *5*−*8*). Base propenals are structural analogues of MDA that are produced during oxidative cleavage of the DNA backbone by agents such as bleomycin, peroxynitrite, or chromium(V) (*9*−*12*). Like MDA, base propenals form M_1G in DNA treated in vitro and are mutagenic in the frameshift tester strain *Salmonella typhimurium hisD3052*. Base propenals are more reactive than MDA in vitro and more mutagenic in vivo (*13*, *14*).

The enol tautomer of MDA, β-hydroxyacrolein, and the base propenals are α,β-unsaturated aldehydes with different leaving groups, but their mechanism of reaction with DNA is similar (Scheme 1). Model chemistry suggests that M_1G is formed by initial 1,2-addition of the exocyclic amino group of guanine to the aldehyde of β-substituted acroleins followed by cyclization with the guanine ring nitrogen (N1) (*15*). Because the N^2 atom of guanine is involved in hydrogen bonding and is buried in the minor groove, the three-dimensional structure of DNA is predicted to impact its reactivity toward α,β-unsaturated aldehydes.

Scheme 1: Formation of M_1G by Malondialdehyde and Base Propenals

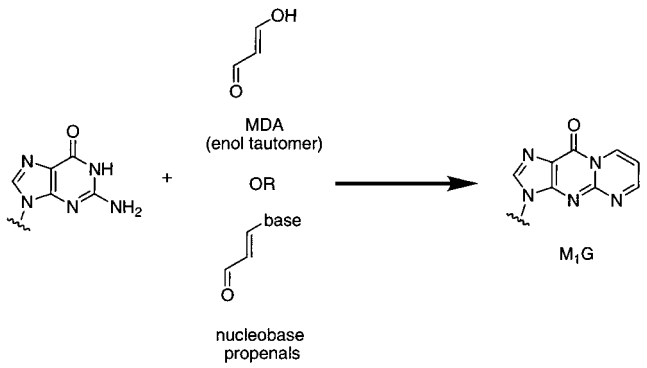

The three-dimensional structure of DNA can vary radically during normal biological processes such as replication, repair, and transcription. For example, during DNA replication, single-stranded and supercoiled intermediates are generated (*16*). RNA transcription involves alteration of nucleosomal structure, DNA bending, and unwinding (*17*−*21*). In addition to biochemically induced structural variations, some tracts of DNA have innately peculiar structure. Particular repetitive sequences can lead to conformations that differ from the canonical B form as described by Dickerson (*22*). Such "defined order sequence" DNA is present in eukaryotic genomes and can exist in bent, A-form, Z-form, hairpin,

† This work was supported by a research grant and center grants from the National Institutes of Health [CA87819, ES00267, CA68485, and GM59790 (P.C.D.)].

* To whom correspondence should be addressed: Department of Biochemistry, Vanderbilt University School of Medicine, Nashville, TN 37232. Fax: (615) 343-7329. E-mail: marnett@toxicology.mc.vanderbilt.edu.

‡ Vanderbilt University School of Medicine.

§ Massachusetts Institute of Technology.

[1] Abbreviations: ECL, enhanced chemiluminescence; DMSO, dimethyl sulfoxide; LC−MS/MS, liquid chromatography−tandem mass spectrometry; MDA, malondialdehyde; M_1G, pyrimido[1,2-*a*]purin-10(3*H*)-one; MNU, *N*-methyl-*N*-nitrosourea; NiCR, 2,12-dimethyl-3,7,11,17-tetraazabicyclo[11.3.1]heptadeca[1(17),2,11,13,15-pentaenato]-nickel(II); PBS, 10 mM phosphate-buffered saline (pH 7.4); PI, propidium iodide; CT, calf thymus; sem, standard error of the mean.

10.1021/bi0113059 CCC: $22.00
Published on Web 03/19/2002

cruciform, triplex, or looped conformations (*23*). Therefore, the structure of genomic DNA is neither static nor homogeneous, and these variations may have important biological consequences, including altered reactivity toward mutagens.

The role of DNA structure in the reaction with mutagens has been briefly explored for certain DNA-damaging agents. For example, the structural changes induced by TATA binding protein direct alkylation at a defined downstream site by pluramycin, an epoxide-containing antitumor antibiotic with intercalating properties (*24*). Additionally, nucleosomal structure has been shown to preferentially direct alkylation by enediynes, dimethylnitrosamine, and aflatoxin B_1 to internucleosomal tracts of DNA (*25*−*27*).

The three-dimensional structure of DNA as dictated by sequence and buffer composition also affects adduct formation. Wurdeman et al. (*28*) treated model DNA substrates that were single-stranded, mismatched, or bulged with *N*-methyl-*N*-nitrosourea (MNU) and 2,12-dimethyl-3,7,11,17-tetraazabicyclo[11.3.1]heptadeca[1(17),2,11,13,15-pentaeneato]nickel(II) (NiCR)/$KHSO_5$. They found that single-stranded DNA is much more sensitive to NiCR/$KHSO_5$ than double-stranded DNA. In the case of MNU, there are less pronounced differences between single- and double-stranded DNA, but the site of alkylation is altered. Mismatched and bulged DNA substrates are more sensitive to damage by NiCR/$KHSO_5$, and the effect on MNU alkylation either increases or decreases depending on sequence. Tang et al. (*29*) examined the effect of Z-DNA structure on DNA damage. They found that guanines in Z-DNA tracts in the context of a plasmid are selectively oxidized by NiCR and Co^{2+} with $KHSO_5$.

The role of topology in directing DNA damage has been explored (*30*, *31*). With regard to strand breaks, oxidizing agents that produce highly reactive intermediates without binding to DNA, such as γ-irradiation and peroxynitrite, are insensitive to differences in superhelical tension. However, some of the oxidizing agents that bind noncovalently to DNA are affected by DNA supercoiling. For example, compared to negatively supercoiled plasmids, positively supercoiled plasmids are more sensitive to oxidation by Cu^{2+}, which binds to DNA and converts H_2O_2 into hydroxyl radical in a site-specific manner (*31*). In addition, the enediyne antibiotic, calicheamicin γ_1^I, damages negatively supercoiled DNA more efficiently than positively supercoiled DNA (*30*). These results show that superhelical tension also can affect the reaction between DNA and damaging agents.

The role of DNA structure in the reaction with α,β-unsaturated aldehydes, such as 4-hydroxynonenal, crotonaldehyde, acrolein, MDA and base propenals, has not been studied. Using MDA and base propenals as model α,β-unsaturated aldehydes, we explored the role of DNA structure on this type of DNA damage in vitro. Specifically, we show that increased levels of exposure of the N^2 atom of guanine in the minor groove by heat denaturation, negative supercoiling, and the addition of simple intercalating agents increases the sensitivity to oxopropenylation. Conversely, this reaction is attenuated in DNA condensed by a high ionic strength or direct blockade of the minor groove.

EXPERIMENTAL PROCEDURES

Reagents. **Caution:** *Ethidium bromide, daunorubicin, doxorubicin, actinomycin D, and 9-aminoacridine should be considered toxic, potential human carcinogens and should be handled accordingly.*

Ethidium bromide, daunorubicin, doxorubicin, distamycin A, and methyl green were purchased from Sigma Chemical Co. Actinomycin D and 9-aminoacridine were purchased from Aldrich. Netropsin was purchased from Fluka (Milwaukee, WI). Plasmid DNA, pBR322, was purchased from Roche Molecular Biochemicals (Mannheim, Germany). *Eco*RI was purchased from New England Biolabs (Beverly, MA). Sodium MDA, adenine propenal, cytosine propenal, and thymine propenal were synthesized according to published methods (*32*, *33*). Products were characterized by ^1H nuclear magnetic resonance using $(CH_3)_2SO$-d_6 as the solvent.

Calf thymus DNA (CT-DNA) was dissolved in 10 mM potassium phosphate buffer (pH 7.0), and aliquots were stored at −20 °C until they were used. Stocks of base propenals were prepared in dimethyl sulfoxide (DMSO) and stored at −20 °C. Sodium MDA stocks were prepared in water just prior to use. Actinomycin D and 9-aminoacridine were dissolved in a water/acetonitrile mixture (10:1, v/v), and distamycin was dissolved in a water/acetonitrile mixture (5:1, v/v). Other DNA binding agents were dissolved in water. Concentrations of stock solutions were determined by UV absorbance using the following extinction coefficients: ethidium bromide (ϵ_{480} = 5850 M^{-1} cm^{-1}) (*34*), daunorubicin, doxorubicin (ϵ_{480} = 11 500 M^{-1} cm^{-1}) (*35*), thymine propenal (ϵ_{304} = 26 900 M^{-1} cm^{-1}), cytosine propenal (ϵ_{314} = 26 800 M^{-1} cm^{-1}), adenine propenal (ϵ_{258} = 34 000 M^{-1} cm^{-1}), and MDA (ϵ_{268} = 34 200 M^{-1} cm^{-1}).

Preparation of DNA Substrates. To generate single- and double-stranded DNA substrates, CT-DNA (0.6 mg/mL) in 10 mM potassium phosphate (pH 7.0) was sonicated for 1 h in a water bath sonicator, incubated in a 100 °C (single-stranded) or room temperature (double-stranded) water bath for 10 min, and immediately cooled on ice until it was used in modification reactions.

To make linearized plasmid DNA, 50 μg of supercoiled pBR322 (0.25 mg/mL) was treated with 125 units of *Eco*RI for 1 h at 37 °C. The supercoiled plasmid was treated similarly, except a 300 mM sodium chloride solution was substituted for the restriction enzyme solution to give similar ionic strengths. Both samples were ethanol precipitated, washed with cold 70% ethanol, and redissolved in 10 mM potassium phosphate (pH 7.0).

Modification of DNA. DNA (0.3 mg/mL) was modified in 100 mM potassium phosphate buffer (pH 7.4) with the indicated concentrations of modifying agents at 37 °C for 24 h. Typically, 20 μg of CT-DNA was employed per treatment, except 450 μg was used for the liquid chromatography−tandem mass spectrometry (LC−MS/MS) study and 10 μg of plasmid DNA was used in the topology study. Reactions run in parallel included the same amount of DMSO (4−8%). For ionic strength studies, 10 mM potassium phosphate buffer was used. DNA binding chemicals were preincubated with DNA for 2 h at room temperature before addition of oxopropenylating agents. Reactions were stopped by addition of $^1/_{10}$ volume of 3 M sodium acetate and 2.5 volumes of cold ethanol followed by storage at −20 °C overnight. The DNA pellet was washed twice with cold 70% ethanol and redissolved to a concentration of 0.1 mg/mL in 10 mM potassium phosphate buffer (pH 7.0) for 1 h at room temperature by mechanical agitation. The M_1G content of

modified DNA samples was determined by immunoslot blot analysis or LC−MS/MS with borohydride reduction as described below.

Immunoslot Blot Analysis of M_1G. Immunoslot blot analysis was carried out as described previously (*14*, *36*). Briefly, DNA samples were immobilized on nitrocellulose membranes, and M_1G content was measured by immunoblot analysis with enhanced chemiluminescence (ECL) using an anti-M_1G monoclonal antibody (*37*). The ECL values were normalized for any variation in the amount of DNA immobilized by subsequently staining membranes with propidium iodide (PI). Relative levels of M_1G in modified DNA samples were expressed as the ratio of ECL signal to PI staining intensity.

Liquid Chromatography−Tandem Mass Spectrometry of Dihydro-M_1G-dR. Modified DNA samples with 33 pmol of isotopically labeled internal standard, [$^2H_2$]M_1G-dR, were enzymatically hydrolyzed to nucleosides and added to 600 μL of an anti-M_1G immunoaffinity gel (*38*). The hydrolysate was diluted to 8 mL with PBS, incubated for 1 h at room temperature with end-over-end mixing, and then poured into a 1 mL extraction tube (Supelco, Bellefonte, PA). The gel was washed with 1 mL of PBS and 1 mL of water. The column was eluted with three 0.5 mL aliquots of methanol into a 2 mL plastic tube. The eluate was evaporated to dryness under reduced pressure, dissolved in 100 μL of water, and stored at −20 °C. Samples were thawed, and 10 μL of a freshly prepared sodium borohydride solution in methanol (10 mg/mL) was added to convert M_1G-dR to the more readily ionized dihydro-M_1G-dR. After incubation for 10 min at room temperature, the reduction reaction was quenched by adding 500 μL of 100 mM ammonium acetate (pH 5.0). The samples were added to 50 mg C_{18} solid-phase extraction tubes (Varian, Palo Alto, CA) and washed with 1 mL of water to remove the excess sodium borohydride. Dihydro-M_1G-dR was eluted with two 0.5 mL aliquots of methanol into a 1.5 mL tube. The eluate was evaporated to dryness under reduced pressure and dissolved in 55 μL of 25 mM ammonium acetate (pH 5.0). The solutions were filtered through 0.22 μm nylon centrifuge tube filters (Corning Costar, Cambridge, MA) by centrifugation and transferred to self-centering glass inserts in autosampler vials for LC−MS/MS analysis. Chromatography was carried out on a Zorbax-C_{18} column (150 mm × 2.1 mm, 5 μm particle size) (Hewlett-Packard, Wilmington, DE) using a Waters 2690 separations module (Waters Corp., Milford, MA). Chromatographic separation was accomplished by increasing the mobile phase from 100% 25 mM ammonium acetate (pH 5.0) to 70% buffer and 30% acetonitrile over the course of 10 min, and then holding at 30% acetonitrile for 10 min. The elution time for dihydro-M_1G-dR was 10 min. The mass spectrometer was a Finnigan MAT TSQ 7000 model (Thermo Finnigan, Bremen, Germany). Electrospray ionization with a voltage of 3.5 kV was employed with 70 psi sheath gas and 20 psi auxiliary gas (N_2). The tube lens voltage and capillary voltage were optimized using a T-unit and direct infusion of a synthetic dihydro-M_1G-dR standard. For selected reaction monitoring analyses, the loss of the deoxyribose moiety (116 mass units) was monitored from the two ions (*m*/*z* 306 and 308) according to dihydro-M_1G-dR and dihydro[$^2H_2$]M_1G-dR with a dwell time of 1 s. The offset voltage was −20 eV for collision-induced dissociation.

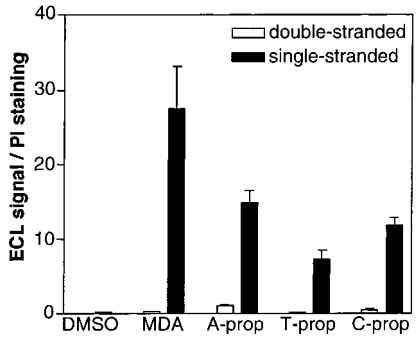

FIGURE 1: Effect of heat denaturation on M_1G formation by MDA and base propenals. Sonicated CT-DNA was either boiled (black bars) or left at ambient temperature (white bars) for 10 min and immediately cooled on ice. DNA (0.3 mg/mL) was incubated with 20 mM sodium malondialdehyde or 0.5 mM base propenal. Reaction mixtures were incubated for 24 h at 37 °C in 100 mM potassium phosphate (pH 7.4). DNA was ethanol precipitated and analyzed by the immunoslot blot method. Bars represent means ± sem ($n = 3$).

Quantitation of M_1G in the original DNA sample was based on the ratio of the peak areas of *m*/*z* 306 and 308 multiplied by the amount of internal standard initially added.

High-Performance Liquid Chromatography of Adenine Propenal and Adenine. To follow conversion of adenine propenal to adenine as stimulated by doxorubicin, high-performance liquid chromatography was employed with a Varian 9012 solvent delivery system (Varian) and ultraviolet detection with a Hewlett-Packard 1040A HPLC detection system (Hewlett-Packard). The column was a Hypersil C_{18} BDS, 5 μm model (2.1 mm × 100 mm) (Hypersil, Needham Heights, MA); the mobile phase was 3% acetonitrile in water, and the flow rate was 0.25 mL/min. Absorbance at 260 nm was followed for both adenine propenal (11 min) and adenine (3 min).

RESULTS

Effect of Base Pairing. To test the effect of Watson−Crick base pairing on susceptibility to modification, we studied differences between single-stranded and double-stranded DNA. Sonicated CT-DNA was heat-denatured and rapidly cooled to generate a single-stranded DNA substrate. Either double-stranded or single-stranded CT-DNA was then treated with 20 mM MDA or 0.5 mM base propenals for 24 h at 37 °C. The reaction time and concentrations were chosen to achieve easily detectable and similar levels of M_1G with all modifying agents (*14*). Relative M_1G levels were quantified by immunoslot blot analysis (Figure 1). Single-stranded DNA was much more sensitive than double-stranded DNA to all the oxopropenylating agents that were tested. The effect of heat denaturation itself on anti-M_1G immunoreactivity was negligible (Figure 1, DMSO). These data suggest that heat denaturation allows access to the N^2 atom of guanine, the nucleophile involved in the initial 1,2-addition to oxopropenylating agents.

Effect of Ionic Strength. Given the anionic character of the phosphodiester backbone, the tertiary structure of DNA is sensitive to variations in ionic strength. To test the role of electrostatic effects on oxopropenylation of DNA, modifications were carried out at various ionic strengths. For these reactions, CT-DNA was treated with oxopropenylating agents in low-ionic strength potassium phosphate buffer (10 mM,

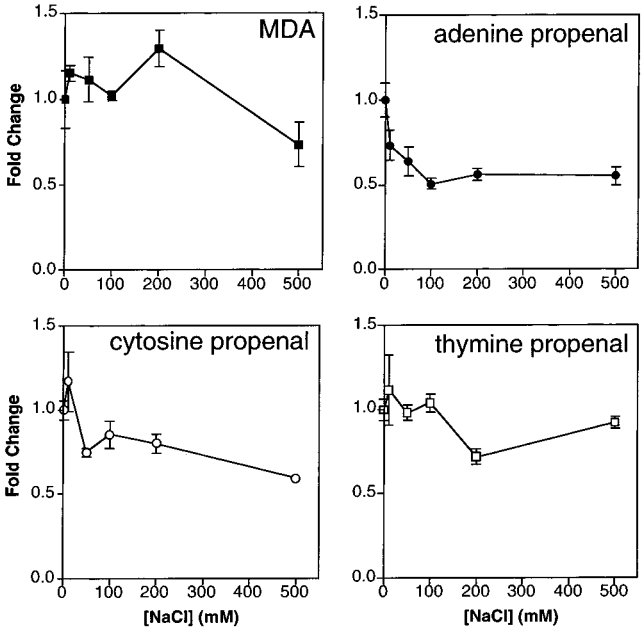

FIGURE 2: Effect of ionic strength on M_1G formation by MDA and base propenals. CT-DNA (0.3 mg/mL) in 10 mM potassium phosphate (pH 7.4) was incubated with various concentrations of sodium chloride and either 40 mM sodium malondialdehyde, 0.25 mM adenine propenal, 0.5 mM thymine propenal, or 0.5 mM cytosine propenal for 24 h at 37 °C. DNA was ethanol precipitated and analyzed by the immunoslot blot method. Values at each concentration represent the mean ± sem normalized to the mean value obtained in the absence of salt ($n = 3$).

compared to 100 mM potassium phosphate for the other reactions) in the presence of increasing sodium chloride concentrations. At high concentrations, sodium chloride inhibited M_1G formation by MDA and cytosine propenal and, to a lesser extent, thymine propenal (Figure 2). In contrast, the level of adenine propenal oxopropenylation was reduced by 50% at salt concentrations of as low as 100 mM, but no more at higher concentrations.

Effect of Plasmid Topology. During normal biological processes such as replication and transcription, DNA is subject to positive and negative supercoiling. We sought to test the effect of DNA topology on oxopropenylation by using a plasmid model. Plasmids grown normally in bacteria are isolated in a negatively supercoiled state. Restriction digestion of a supercoiled plasmid at a single site results in a relaxed, linearized plasmid. We modified linearized and mock-digested pBR322 with MDA and base propenals. As can be seen in Figure 3, supercoiled plasmid DNA was more sensitive to oxopropenylation than relaxed, linearized plasmid DNA.

Effect of Intercalation. We originally hypothesized that the enhanced reactivity of base propenals compared to MDA was in part due to formation of an intercalated intermediate. To test this hypothesis, we attempted to compete for binding sites with the classic intercalator, ethidium bromide (Figure 4). Rather than observing a concentration-dependent decrease in DNA modification by base propenals, we found the level of oxopropenylation was dramatically increased by ethidium bromide. Unlike other reports of intercalator-enhanced alkylation of ~30%, we observed enhancements of 400−1200% (*39*).

Because the enhancement of oxopropenylation by ethidium bromide was unexpected and dramatic, we sought to confirm

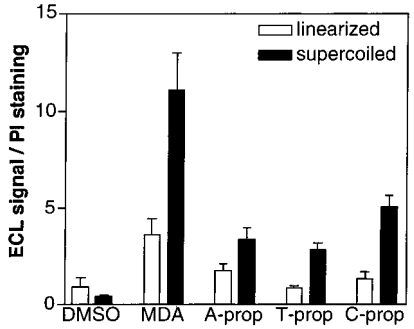

FIGURE 3: Effect of DNA topology on M_1G formation by MDA and base propenals. Negatively supercoiled plasmid DNA was either linearized by *Eco*RI digestion (white bars) or mock treated (black bars). Plasmid (0.3 mg/mL) was incubated with 40 mM sodium malondialdehyde, 0.25 mM adenine propenal, 0.5 mM thymine propenal, or 0.5 mM cytosine propenal. Reaction mixtures were incubated for 24 h at 37 °C in 100 mM potassium phosphate (pH 7.4). DNA was ethanol precipitated and analyzed by the immunoslot blot method. Bars represent means ± sem ($n \geq 3$).

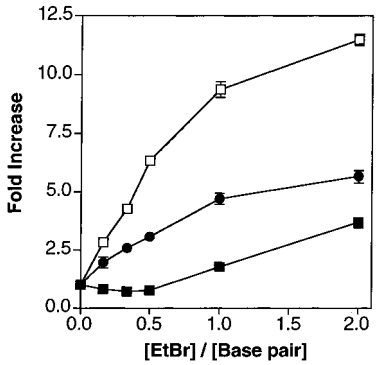

FIGURE 4: Effect of ethidium bromide on M_1G formation by MDA and base propenals. DNA (0.3 mg/mL, 460 μM base pairs) was preincubated with various concentrations of ethidium bromide and modified with 25 mM MDA (■), 0.5 mM adenine propenal (●), or 0.5 mM thymine propenal (□) for 24 h at 37 °C. Samples were analyzed by the immunoslot blot method (ECL only). The ECL signals of MDA and thymine propenal-treated DNA in the absence of ethidium bromide were 70 and 50% lower, respectively, than that for adenine propenal. Values at each concentration represent the mean ± sem normalized to the mean value obtained in the absence of an intercalating agent ($n = 3$).

the result. One hypothesis to explain this finding was that the enhancement was simply an artifact of the immunoslot blot method whereby ethidium remaining bound to the DNA would somehow lead to increased immunoreactivity. This hypothesis was tested by deliberately adding ethidium bromide to standard curve samples prior to immunoslot blot analysis (Figure 5). Clearly, ethidium bromide actually *decreased* immunoslot blot sensitivity, suggesting that the observed enhancement was not an artifact of the assay. However, to confirm that the enhancement of M_1G formation by ethidium bromide was genuine, an alternate analytical method, namely, LC−MS/MS, was employed. CT-DNA (450 μg) was modified with adenine propenal or thymine propenal in the presence of ethidium bromide. Subsequently, 3 μg of the sample was analyzed by the immunoslot blot method, and the remainder was subject to LC−MS/MS analysis (Figure 6). In the latter method, M_1G was separated from any residual ethidium bromide by DNA hydrolysis and immunoaffinity purification. The resulting M_1G-dR was reduced to dihydro-M_1G-dR with sodium borohydride and quantified by stable isotope dilution LC−MS/MS. Both

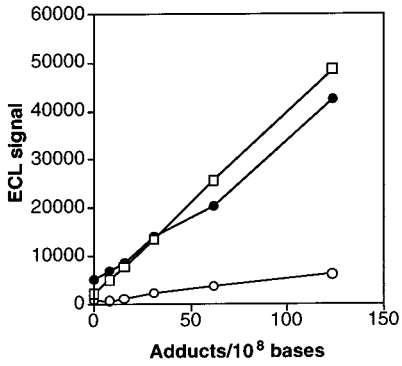

FIGURE 5: Effect of ethidium bromide on immunoslot blot analysis. MDA-modified CT-DNA was diluted with unmodified CT-DNA to various adduct concentrations and analyzed by the immunoslot blot method in the absence (□) or presence of 100 (●) or 500 μM (○) ethidium bromide. The ECL signal is plotted against adduct level ($n = 1$).

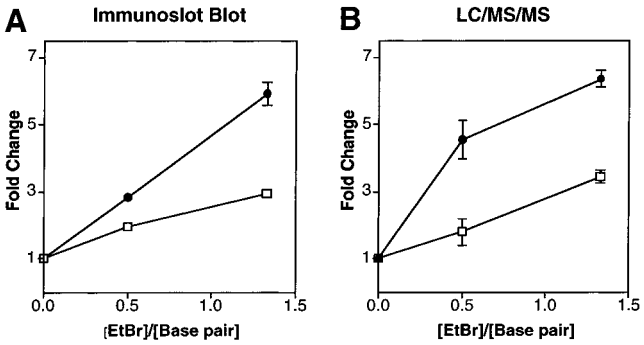

FIGURE 6: LC−MS/MS and immunoslot blot analysis of DNA modified by base propenals in the presence of ethidium bromide. DNA (0.45 mg/mL, 690 μM base pairs) was preincubated with various concentrations of ethidium bromide and modified with 0.5 mM adenine propenal (●) or thymine propenal (□) for 24 h at 37 °C. Samples were divided and analyzed by (A) the immunoslot blot method (ECL only) or (B) LC−MS/MS (reduction method). Values represent the mean ± sem normalized to the mean value obtained in the absence of ethidium bromide ($n = 2$).

methods of M_1G analysis gave similar results, suggesting that the enhancement of oxopropenylation by ethidium bromide was authentic. This effect is likely due to a general unwinding of the DNA, which presumably allows greater access to the N^2 atom of guanine.

To further characterize this effect, other molecules that specifically bind DNA were tested (Figure 7). Figure 8 shows the effect of additional intercalating agents on oxopropenylation by MDA and adenine propenal. Acridine dyes are simple tricycles, which bind to DNA because they are planar molecules that are protonated at neutral pH (Figure 7). A representative acridine dye, 9-aminoacridine, stimulated oxopropenylation by MDA and adenine propenal 2−3-fold, respectively [Figure 8 (○)]. This pattern was similar to that for ethidium, which is consistent with their similar binding affinities and modes of DNA interaction.

Actinomycin D is a complex intercalator with a tricyclic phenoxazone group and two cyclopeptide lactone substituents that cover four base pairs in the minor groove promoting very tight binding (Figure 7). The binding constant (K) for binding of actinomycin D to DNA is 3.8×10^6 M^{-1}, whereas the K of ethidium is 0.1×10^6 M^{-1} (*40*). Unlike 9-aminoacridine, actinomycin D decreased the level of oxopropenylation by MDA and adenine propenal [Figure 8 (■)]. This suggests that the dominant effect is blockade of the minor groove by the cyclopeptide substituents.

The anthracycline anticancer drugs daunorubicin and doxorubicin have an intercalating anthraquinone moiety linked to a minor groove-binding daunosamine sugar (Figure 7) (*41*). At lower concentrations, both drugs stimulated oxopropenylation by both MDA and adenine propenal (Figure 9). However, at higher concentrations of anthracycline drugs, the enhancement of the adenine propenal reaction was attenuated. At the highest concentrations, the amount of oxopropenylation with adenine propenal was actually decreased. This decrease could be attributed to inactivation of adenine propenal by the anthracycline drugs by virtue of their reactive primary amine groups (Figure 7). At low concentrations of anthracycline drugs, most of the drug is bound to DNA, altering DNA structure for efficient oxopropenylation in a manner similar to that of ethidium bromide and 9-aminoacridine. However, at high concentrations, free anthracycline drug could react with the oxopropenylating agent, attenuating modification. Incubating adenine propenal with doxorubicin stimulated the conversion of adenine propenal to adenine as assessed by high-performance liquid chromatography with ultraviolet detection (Figure 10). This suggests that the decrease at high anthracycline concentrations observed in Figure 9B is due to a direct reaction between adenine propenal and the drugs. MDA oxopropenylation was not similarly affected due to its overwhelming excess (50 mM) compared to anthracycline drug concentrations.

Effect of Minor and Major Groove Binding. The effect of various groove-binding agents on oxopropenylation by MDA and adenine propenal was explored (Figure 11). Netropsin and distamycin are structurally related crescent-shaped molecules with a high affinity for the minor groove of AT-rich sequences. Both modestly inhibited oxopropenylation, suggesting that shielding the minor groove can block access to the N^2 atom of guanine and therefore modification.

There are few reported small molecules that bind DNA in the major groove. One exception is methyl green, which appears to participate in groove binding in general as shown by linear dichroism, but it is excluded from triplex DNA, where the third strand lies in the major groove (*42*). These findings have been interpreted as selective major groove binding, but others have suggested that other binding modalities are possible (*43*). Nevertheless, methyl green did not dramatically affect oxopropenylation by either MDA or adenine propenal [Figure 11 (□)]. This further supports the idea that oxopropenylating agents approach the DNA nucleophile by way of the minor groove and not the major groove.

DISCUSSION

MDA, a product of lipid peroxidation, and base propenals, products of DNA backbone oxidation, react with DNA to form M_1G adducts. The results presented here characterize the role of target DNA structure in these reactions. MDA and base propenals modify single-stranded DNA more effectively than double-stranded DNA, and supercoiled plasmid DNA more than relaxed plasmid DNA. A high ionic strength inhibits oxopropenylation to some extent, especially by adenine propenal. Unwinding of target DNA with simple

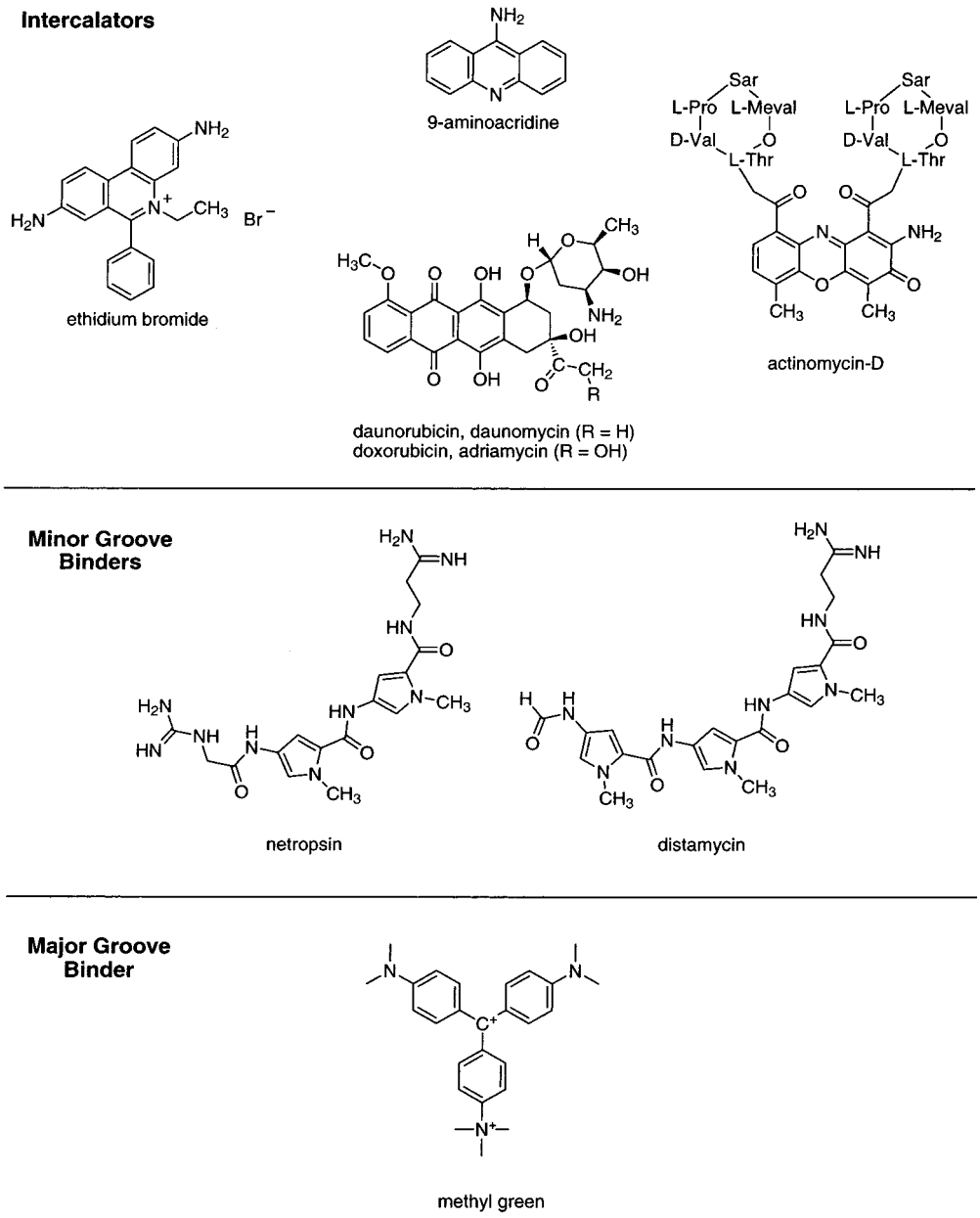

FIGURE 7: Structures of DNA binding agents used in this study.

intercalating agents enhances oxopropenylation severalfold, but blockade of the minor groove attenuates oxopropenylation. These results suggest that oxopropenylation requires steric access to the reaction site, which lies in the minor groove.

Steric Hindrance and Oxopropenylation. Increasing ionic strength affects DNA structure by reducing the electrostatic repulsion between the negatively charged backbones, which allows for a more compact helix. High salt concentrations have variable effects on DNA damage reactions. Reactions of electrophiles that intercalate prior to covalent binding are normally inhibited by high salt concentrations. For example, reactions of polycyclic aromatic hydrocarbon diol epoxides are quite sensitive to salt concentration (*44*). Presumably, the more compact helix disfavors opening of intercalation sites. Alkylation by nitrosamines such as MNU is also inhibited by increasing ionic strengths (*39*, *45*). This has been explained by interruption of the electrostatic attraction between the cationic alkylating intermediate, diazonium ion, and the anionic DNA target. In contrast, neither salt nor cationic DNA binders (spermine and ethidium) affect reactivity of the small, neutral alkylating agent, dimethyl sulfate (*45*, *46*).

High salt had a modest inhibitory effect on all the oxopropenylating agents that were tested, but oxopropenylation by adenine propenal was the most sensitive. If we assume that adenine propenal is not charged when it reacts with DNA, attenuation of favorable electrostatic interactions probably does not explain the inhibitory effect. The simplest hypothesis is that high salt compacts the DNA helix, reducing steric access to the DNA nucleophile. Because adenine propenal is the bulkiest oxopropenylating agent, it is most sensitive to this effect.

We attempted to test the hypothesis that intercalation by adenine propenal is required for its reaction with DNA by competition with a known intercalating agent, ethidium bromide. This approach was based on similar experiments by Gopalakrishnan et al. (*47*), who demonstrated that

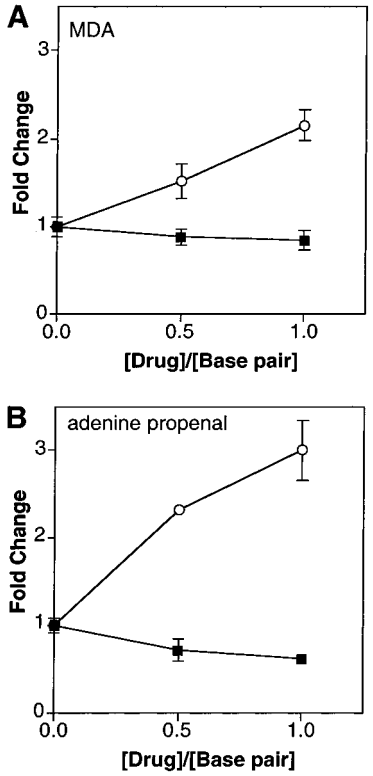

FIGURE 8: Effect of 9-aminoacridine and actinomycin D on M_1G formation by MDA and adenine propenal. DNA (0.3 mg/mL, 460 μM base pairs) was preincubated with 0.5 and 1 base pair equivalents of 9-aminoacridine (○) or actinomycin D (■) and modified with (A) 50 mM MDA or (B) 0.25 mM adenine propenal for 24 h at 37 °C. Samples were analyzed by the immunoslot blot method. Because some of the drugs have electronic properties that can interfere with fluorescence quantitation of propidium iodide staining, the ECL signals alone were used. The ECL signal of adenine propenal-treated DNA in the absence of intercalating agents was 27% lower than that for MDA. Values at each concentration represent the mean ± sem normalized to the mean value obtained in the absence of intercalating agent ($n = 3$).

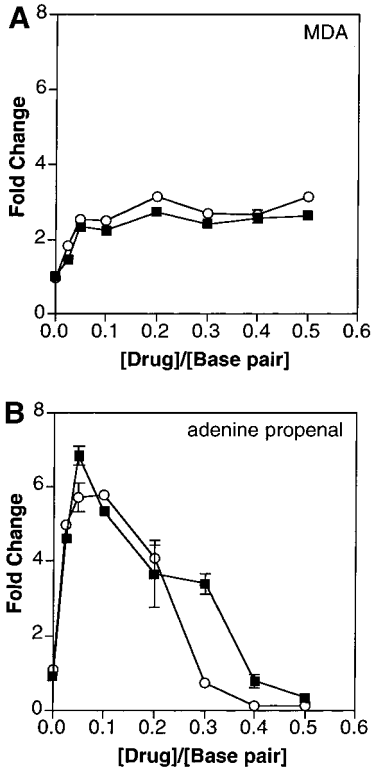

FIGURE 9: Concentration-dependent effect of anthracycline drugs on M_1G formation by MDA and adenine propenal. DNA (0.3 mg/mL, 460 μM base pairs) was preincubated with varying concentrations of daunorubicin (■) or doxorubicin (○) and modified with (A) 50 mM MDA or (B) 0.25 mM adenine propenal for 24 h at 37 °C. Samples were analyzed by the immunoslot blot method. Because these drugs have electronic properties that can interfere with fluorescence quantitation of propidium iodide staining, only ECL signals were calculated. The ECL signal of adenine propenal-treated DNA in the absence of intercalating agents was 48% lower than that for MDA. Values at each concentration represent the mean ± sem normalized to the mean value obtained in the absence of drug ($n = 3$).

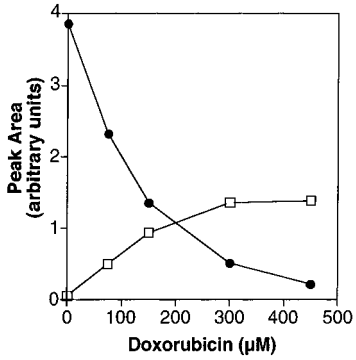

FIGURE 10: Concentration-dependent conversion of adenine propenal to adenine by doxorubicin. An aqueous solution of adenine propenal (10 μM) was incubated with various concentrations of doxorubicin at 37 °C for 16 h. Relative levels of adenine propenal (●) and adenine (□) were determined by high-performance liquid chromatography analysis by monitoring A_{260}. The column was a Hypersil C_{18} BDS, 5 μm model (2.1 mm × 100 mm), and the mobile phase was 3% acetonitrile in water. The retention times were 3 min for adenine and 11 min for adenine propenal. The peak areas are plotted against the concentration of doxorubicin ($n = 1$).

ethidium could compete with intercalation of aflatoxin B_1 and its subsequent modification of N7 of guanine. Contrary to expectations, a dramatic enhancement in oxopropenylation was observed, suggesting that intercalation of base propenals is not an important factor in reactivity. The magnitude of the enhancement was unexpected because other alkylating agents are either inhibited (MNU) or not affected (dimethyl sulfate) by ethidium (*39*, *45*). One exception is a conjugate of MNU linked to the intercalator phenyl neutral red; alkylation at the N7 atom of guanine was enhanced ~30% by 500 μM ethidium bromide, but this is a modest effect compared to the severalfold differences observed with oxopropenylating agents (*39*). These differences between oxopropenylation and alkylation by MNU and dimethyl sulfate might be explained by the sites of reactivity. MNU and dimethyl sulfate react mainly with the relatively solvent exposed N7 atom of guanine and N7 and N3 atoms of adenine. In contrast, formation of M_1G begins with modification of the less sterically accessible N^2 atom of guanine. Because it is buried in the minor groove and is involved in hydrogen bonding in base-paired DNA, its reactivity may be uniquely sensitive to structural changes induced by increasing ionic strengths and intercalation. As the ionic strength increases, the DNA helix becomes more compact, and the N^2 atom of guanine becomes less accessible. In contrast, as intercalating agents expand the stacked bases, the helix unwinds and makes the N^2 atom of guanine more accessible (*48*, *49*). Alternately, intercalating agents may decrease steric hindrance by rapidly exchanging between

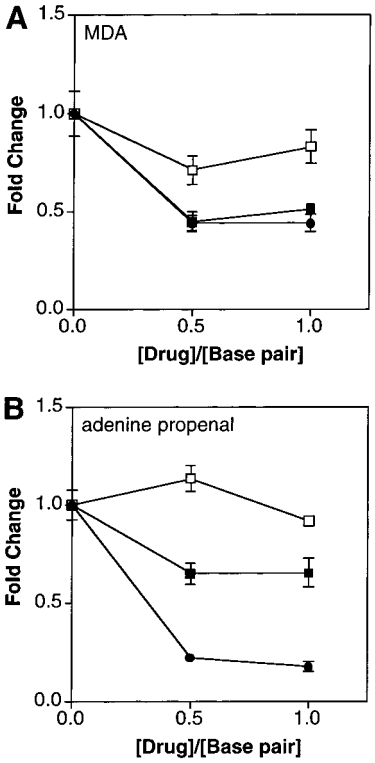

FIGURE 11: Effect of various DNA groove binding agents on M_1G formation by MDA and adenine propenal. DNA (0.3 mg/mL, 460 μM base pairs) was preincubated with 0.5 and 1 base pair equivalents of netropsin (■), distamycin (●), or methyl green (□) and modified with (A) 50 mM MDA or (B) 0.25 mM adenine propenal for 24 h at 37 °C. Samples were analyzed by the immunoslot blot method (ECL signal only). The ECL signal of adenine propenal-treated DNA in the absence of intercalating agents was 27% lower than that for MDA. Values at each concentration represent the mean ± sem normalized to the mean value obtained in the absence of groove binding agent ($n = 3$).

solvent and DNA binding sites, leaving transient gaps between the stacked bases. These short-lived gaps might allow oxopropenylating agents to slip between base pairs and attack N^2 from above or below the base pair plane, minimizing steric clash with hydrogen bonding atoms.

Minor Groove Effects. Kelly et al. (*50*) showed that formation of the minor groove adducts N^3-methyladenine and N^3-methylguanine by methyl methanesulfonate and MNU is inhibited by the minor groove binder distamycin, whereas formation of the major groove adduct N^7-methylguanine is unaffected. These data are consistent with our observations that the minor groove binders distamycin and netropsin attenuated M_1G formation but that the major groove binder methyl green did not. Because the binding specificity of methyl green has not been completely elucidated, these results need to be interpreted cautiously.

Using chromatin DNA as a substrate, Rajalakshmi et al. (*51*) demonstrated a more general inhibition by distamycin of MNU-induced adducts at the N7 and O^6 positions of guanine and the N3 position of adenine. They argue that distamycin selectively binds A-T tracts and prevents local melting, thereby stabilizing base pairing in general. The greatly enhanced sensitivity of melted DNA to oxopropenylation indicates that a similar mechanism may also play a role here.

Actinomycin D is a unique compound in that its interaction with DNA has significant minor groove binding and intercalative components. Inhibition of oxopropenylation by actinomycin D can be explained by the two large cyclopeptide lactone groups that bidirectionally lie in the minor groove and block access to the N^2 atom of guanine in a manner similar to that of netropsin and distamycin. Daunorubicin and doxorubicin also have both intercalating and minor groove binding elements, but compared with actinomycin D, the minor groove binding moiety is unidirectional and relatively small. On the basis of the observation that the anthracycline drugs enhanced oxopropenylation, it seems that exposure of the N^2 atom of guanine by helix unwinding dominates any minor groove blocking effect.

CONCLUSION

We have shown that the structure of DNA dramatically impacts the sensitivity to adduct formation by the α,β-unsaturated aldehydes MDA and base propenals. The nucleophile involved in oxopropenylation, the N^2 atom of guanine, lies at the floor of the minor groove and is relatively hindered compared to other reactive sites in DNA. For this reason, conditions that block access to the minor groove, such as helix compression by increased ionic strength or minor groove binding agents, inhibit oxopropenylation. In contrast, conditions that increase the level of exposure of N^2, such as unwinding by intercalators or strand melting, increase the extent of oxopropenylation. The role of DNA structure in the reactivity of oxopropenylating agents can likely be generalized to other α,β-unsaturated aldehydes that react with the N^2 atom of guanine. Such observations are important in understanding the interactions between processes that modulate DNA structure and DNA-damaging agents.

ACKNOWLEDGMENT

We thank J. Scott Daniels, Kent Gates, Chiara Leuratti, and Carol Rouzer for helpful discussions.

REFERENCES

1. Spalding, J. W. (1988) Toxicology and carcinogenesis studies of malondialdehyde sodium salt (3-hydroxy-2-propenal, sodium salt) in F344/N rats and B6C3F1 mice, *Natl. Toxicol. Porgram Tech. Rep. Ser. 331*, 5−13.
2. Basu, A. K., and Mamett, L. J. (1983) Unequivocal demonstration that malondialdehyde is a mutagen, *Carcinogenesis 4*, 331−333.
3. Yau, T. M. (1979) Mutagenicity and cytotoxicity of malondialdehyde in mammalian cells, *Mech. Ageing Dev. 11*, 137−144.
4. Marnett, L. J., Hurd, H. K., Hollstein, M. C., Levin, D. E., Esterbauer, H., and Ames, B. N. (1985) Naturally occurring carbonyl compounds are mutagens in *Salmonella* tester strain TA104, *Mutat. Res. 148*, 25−34.
5. Seto, H., Okuda, T., Takesue, T., and Ikemura, T. (1983) Reaction of malondialdehyde with nucleic acid. I. Formation of fluorescent pyrimido[1,2-*a*]purin-10(3*H*)-one nucleosides, *Bull. Chem. Soc. Jpn. 56*, 1799−1802.
6. Stone, K., Ksebati, M., and Marnett, L. J. (1990) Investigation of the adducts formed by reaction of malondialdehyde with adenosine, *Chem. Res. Toxicol. 3*, 33−38.
7. Nair, V., Turner, G. A., and Offerman, R. J. (1984) Novel adducts from the modification of nucleic acid bases by malondialdehyde, *J. Am. Chem. Soc. 106*, 3370−3371.
8. Basu, A. K., O'Hara, S. M., Valladier, P., Stone, K., Mols, O., and Marnett, L. J. (1988) Identification of adducts formed by reaction of guanine nucleosides with malondialdehyde and structurally related aldehydes, *Chem. Res. Toxicol. 1*, 53−59.

9. Giloni, L., Takeshita, M., Johnson, F., Iden, C., and Grollman, A. P. (1981) Bleomycin-induced strand-scission of DNA. Mechanism of deoxyribose cleavage, *J. Biol. Chem. 256*, 8608−8615.
10. Sugden, K. D., and Wetterhahn, K. E. (1996) Identification of the oxidized products formed upon reaction of chromium-(V) with thymidine nucleotides, *J. Am. Chem. Soc. 118*, 10811−10818.
11. Yermilov, V., Yoshie, Y., Rubio, J., and Ohshima, H. (1996) Effects of carbon dioxide/bicarbonate on induction of DNA single-strand breaks and formation of 8-nitroguanine, 8-oxoguanine and base-propenal mediated by peroxynitrite, *FEBS Lett. 399*, 67−70.
12. Sugden, K. D., and Wetterhahn, K. E. (1997) Direct and hydrogen peroxide-induced chromium(V) oxidation of deoxyribose in single-stranded and double-stranded calf thymus DNA, *Chem. Res. Toxicol. 10*, 1397−1406.
13. Dedon, P. C., Plastaras, J. P., Rouzer, C. A., and Marnett, L. J. (1998) Indirect mutagenesis by oxidative DNA damage: formation of the pyrimidopurinone adduct of deoxyguanosine by base propenal, *Proc. Natl. Acad. Sci. U.S.A. 95*, 11113−11116.
14. Plastaras, J. P., Riggins, J. N., Otteneder, M., and Marnett, L. J. (2000) Reactivity and mutagenicity of endogenous DNA oxopropenylating agents: base propenals, malondialdehyde, and N^{ϵ}-oxopropenyllysine, *Chem. Res. Toxicol. 13*, 1235−1242.
15. Reddy, G. R., and Mamett, L. J. (1996) Mechanism of reaction of β-(aryloxy)acroleins with nucleosides, *Chem. Res. Toxicol. 9*, 12−15.
16. Postow, L., Peter, B. J., and Cozzarelli, N. R. (1999) Knot what we thought before: the twisted story of replication, *BioEssays 21*, 805−808.
17. Kornberg, R. D. (1999) Eukaryotic transcriptional control, *Trends Cell Biol. 9*, M46−M49.
18. Kahn, J. D. (2000) Topological effects of the TATA box binding protein on minicircle DNA and a possible thermodynamic linkage to chromatin remodeling, *Biochemistry 39*, 3520−3524.
19. Kim, Y., Geiger, J. H., Hahn, S., and Sigler, P. B. (1993) Crystal structure of a yeast TBP/TATA-box complex, *Nature 365*, 512−520.
20. Coulombe, B., and Burton, Z. F. (1999) DNA bending and wrapping around RNA polymerase: a "revolutionary" model describing transcriptional mechanisms, *Microbiol. Mol. Biol. Rev. 63*, 457−478.
21. Liu, L. F., and Wang, J. C. (1987) Supercoiling of the DNA template during transcription, *Proc. Natl. Acad. Sci. U.S.A. 84*, 7024−7027.
22. Wing, R., Drew, H., Takano, T., Broka, C., Tanaka, S., Itakura, K., and Dickerson, R. E. (1980) Crystal structure analysis of a complete turn of B-DNA, *Nature 287*, 755−758.
23. Sinden, R. R., Hashem, V. I., and Rosche, W. A. (1999) DNA-directed mutations. Leading and lagging strand specificity, *Ann. N.Y. Acad. Sci. 870*, 173−189.
24. Sun, D., and Hurley, L. H. (1995) TBP binding to the TATA box induces a specific downstream unwinding site that is targeted by pluramycin, *Chem. Biol. 2*, 457−469.
25. Bailey, G. S., Nixon, J. E., Hendricks, J. D., Sinnhuber, R. O., and Van Holde, K. E. (1980) Carcinogen aflatoxin B1 is located preferentially in internucleosomal deoxyribonucleic acid following exposure in vivo in rainbow trout, *Biochemistry 19*, 5836−5842.
26. Ramanathan, R., Rajalakshmi, S., Sarma, D. S., and Farber, E. (1976) Nonrandom nature of in vivo methylation of dimethylnitrosamine and the subsequent removal of methylated products from rat liver chromatin DNA, *Cancer Res. 36*, 2073−2079.
27. Wu, J., Xu, J., and Dedon, P. C. (1999) Modulation of enediyne-induced DNA damage by chromatin structures in transcriptionally active genes, *Biochemistry 38*, 15641−15646.
28. Wurdeman, R. L., Douskey, M. C., and Gold, B. (1993) DNA methylation by *N*-methyl-*N*-nitrosourea: methylation pattern changes in single- and double-stranded DNA, and in DNA with mismatched or bulged guanines, *Nucleic Acids Res. 21*, 4975−4980.
29. Tang, N., Muller, J. G., Burrows, C. J., and Rokita, S. E. (1999) Nickel and cobalt reagents promote selective oxidation of Z-DNA, *Biochemistry 38*, 16648−16654.
30. LaMarr, W. A., Yu, L., Nicolaou, K. C., and Dedon, P. C. (1998) Supercoiling affects the accessibility of glutathione to DNA-bound molecules: positive supercoiling inhibits calicheamicin-induced DNA damage, *Proc. Natl. Acad. Sci. U.S.A. 95*, 102−107.
31. LaMarr, W. A., Sandman, K. M., Reeve, J. N., and Dedon, P. C. (1997) Differential effects of DNA supercoiling on radical-mediated DNA strand breaks, *Chem. Res. Toxicol. 10*, 1118−1122.
32. Johnson, F., Pillai, K. M., Grollman, A. P., Tseng, L., and Takeshita, M. (1984) Synthesis and biological activity of a new class of cytotoxic agents: *N*-(3-oxoprop-1-enyl)-substituted pyrimidines and purines, *J. Med. Chem. 27*, 954−958.
33. Marnett, L. J., Bienkowski, M. J., Raban, M., and Tuttle, M. A. (1979) Studies of the hydrolysis of ^{14}C-labeled tetraethoxypropane to malondialdehyde, *Anal. Biochem. 99*, 458−463.
34. Bresloff, J. L., and Crothers, D. M. (1975) DNA-ethidium reaction kinetics: demonstration of direct ligand transfer between DNA binding sites, *J. Mol. Biol. 95*, 103−123.
35. Frezard, F., and Garnier-Suillerot, A. (1990) Comparison of the binding of anthracycline derivatives to purified DNA and to cell nuclei, *Biochim. Biophys. Acta 1036*, 121−127.
36. Leuratti, C., Singh, R., Lagneau, C., Farmer, P. B., Plastaras, J. P., Marnett, L. J., and Shuker, D. E. (1998) Determination of malondialdehyde-induced DNA damage in human tissues using an immunoslot blot assay, *Carcinogenesis 19*, 1919−1924.
37. Sevilla, C. L., Mahle, N. H., Eliezer, N., Uzieblo, A., O'Hara, S. M., Nokubo, M., Miller, R., Rouzer, C. A., and Marnett, L. J. (1997) Development of monoclonal antibodies to the malondialdehyde-deoxyguanosine adduct, pyrimidopurinone, *Chem. Res. Toxicol. 10*, 172−180.
38. Rouzer, C. A., Chaudhary, A. K., Nokubo, M., Ferguson, D. M., Reddy, G. R., Blair, I. A., and Marnett, L. J. (1997) Analysis of the malondialdehyde-2′-deoxyguanosine adduct pyrimidopurinone in human leukocyte DNA by gas chromatography/electron capture/negative chemical ionization/mass spectrometry, *Chem. Res. Toxicol. 10*, 181−188.
39. Mehta, P., Church, K., Williams, J., Chen, F. X., Encell, L., Shuker, D. E., and Gold, B. (1996) The design of agents to control DNA methylation adducts. Enhanced major groove methylation of DNA by an *N*-methyl-*N*-nitrosourea functionalized phenyl neutral red intercalator, *Chem. Res. Toxicol. 9*, 939−948.
40. Chaires, J. B. (1997) Energetics of drug−DNA interactions, *Biopolymers 44*, 201−215.
41. Nunn, C. M., Van Meervelt, L., Zhang, S. D., Moore, M. H., and Kennard, O. (1991) DNA-drug interactions. The crystal structures of d(TGTACA) and d(TGATCA) complexed with daunomycin, *J. Mol. Biol. 222*, 167−177.
42. Kim, S. K., and Norden, B. (1993) Methyl green. A DNA major-groove binding drug, *FEBS Lett. 315*, 61−64.
43. Durand, M., Gondeua, C., and Maurizot, J. C. (1998) Interaction of methyl green with an oligonucleotide in intramolecular duplex and triplex conformations, *Eur. Biophys. J. 27*, 147−151.
44. Fernando, H., Huang, C. R., Milliman, A., Shu, L., and LeBreton, P. R. (1996) Influence of Na^+ on DNA reactions with aromatic epoxides and diol epoxides: evidence that DNA catalyzes the formation of benzo[*a*]pyrene and benz[*a*]anthracene adducts at intercalation sites, *Chem. Res. Toxicol. 9*, 1391−1402.
45. Wurdeman, R. L., and Gold, B. (1988) The effect of DNA sequence, ionic strength, and cationic DNA affinity binders on the methylation of DNA by *N*-methyl-*N*-nitrosourea, *Chem. Res. Toxicol. 1*, 146−147.
46. Rajalakshmi, S., Rao, R. M., and Sarma, D. S. (1980) Carcinogen-DNA interaction: differential effects of distamycin-A and spermine on the formation of 7-methylguanine in

DNA by *N*-methyl-*N*-nitrosourea, methylmethanesulfonate, and dimethylsulfate, *Teratog., Carcinog., Mutagen. 1*, 97−104.
47. Gopalakrishnan, S., Byrd, S., Stone, M. P., and Harris, T. M. (1989) Carcinogen-nucleic acid interactions: equilibrium binding studies of aflatoxin B1 with the oligodeoxynucleotide $d(ATGCAT)_2$ and with plasmid pBR322 support intercalative association with the B-DNA helix, *Biochemistry 28*, 726−734.
48. Jain, S. C., Tsai, C. C., and Sobell, H. M. (1977) Visualization of drug-nucleic acid interactions at atomic resolution. II. Structure of an ethidium/dinucleoside monophosphate crystalline complex, ethidium:5-iodocytidylyl (3′−5′) guanosine, *J. Mol. Biol. 114*, 317−331.
49. Tsai, C. C., Jain, S. C., and Sobell, H. M. (1977) Visualization of drug-nucleic acid interactions at atomic resolution. I. Structure of an ethidium/dinucleoside monophosphate crystalline complex, ethidium:5-iodouridylyl (3′−5′) adenosine, *J. Mol. Biol. 114*, 301−315.
50. Kelly, J. D., Shah, D., Chen, F. X., Wurdeman, R., and Gold, B. (1998) Quantitative and qualitative analysis of DNA methylation at N3-adenine by *N*-methyl-*N*-nitrosourea, *Chem. Res. Toxicol. 11*, 1481−1486.
51. Rajalakshmi, S., Rao, P. M., and Sarma, D. S. (1978) Studies on carcinogen chromatin−DNA interaction: inhibition of *N*-methyl-*N*-nitrosourea-induced methylation of chromatin−DNA by spermine and distamycin A, *Biochemistry 17*, 4515−4518.

BI0113059